An Interactive Computer Graphics Study of Thermolysin-Catalyzed Peptide Cleavage and Inhibition by *N*-Carboxymethyl Dipeptides†

David G. Hangauer,* Arthur F. Monzingo, and Brian W. Matthews

ABSTRACT: Interactive computer graphics was used as a tool in studying the cleavage mechanism of the model substrate Z-Phe-Phe-Leu-Trp by the zinc endopeptidase thermolysin. Two Michaelis complexes and three binding orientations of the tetrahedral intermediate to the crystal structure of thermolysin were investigated. Our results indicate that a Michaelis complex, which does not involve coordination of the scissile peptide to the zinc, is consistent with available experimental data and the most plausible of the two complexes. A tetrahedral intermediate complex wherein the two oxygens of the hydrated scissile peptide straddle the zinc in a bidentate fashion results in the most favorable interactions with the active site. The preferred tetrahedral intermediate and Michaelis complex provide a rationalization for the published substrate data. A trajectory for proceeding from the Michaelis complex to the tetrahedral intermediate is proposed. This trajectory involves a simultaneous activation of the zinc-bound water molecule concurrent with attack on the scissile peptide. A detailed ordered product release mechanism is also presented. These studies suggest some modifications and a number of extensions to the mechanism proposed earlier [Kester, W. R., & Matthews, B. W. (1977) *Biochemistry 16*, 2506; Holmes, M. A., & Matthews, B. W. (1981) *Biochemistry 20*, 6912]. The binding mode of the thermolysin inhibitor *N*-(1-carboxy-3-phenylpropyl)-L-leucyl-L-tryptophan [Monzingo, A. F., & Matthews, B. W. (1984) *Biochemistry* (preceding paper in this issue)] is compared with that of the preferred tetrahedral intermediate, providing insight into this inhibitor design.

Interactive computer graphics is emerging as a powerful tool for studying the molecular interactions of macromolecules with ligands (Meyer, 1980; Langridge et al., 1981). Several recent reports have demonstrated the synergistic use of this tool with quantitative structure–activity relationships (Hansch et al., 1982; Smith et al., 1982) and molecular mechanics calculations (Blaney et al., 1982a; Wipff et al., 1983). Interactive computer graphics has also been used to rank the binding affinities of some previously untested thyroxine analogues to prealbumin, which were subsequently verified by experiment (Blaney et al., 1982b).

In the present investigation we have applied this tool to studying the mechanism of peptide hydrolysis by the zinc endopeptidase thermolysin (TLN).[1] This enzyme is particularly suited for such a study because a variety of crystallographic, inhibitor, substrate, and chemical modification data are available. Importantly, the crystal and solution conformations appear to be very similar on the basis of available experimental comparisons (Horrocks & Sudnick, 1981) and the finding that the crystalline enzyme still hydrolyzes peptides (Holmes & Matthews, 1981). The relevance of the crystal structure is further enhanced by the fact that thermolysin changes very little upon binding numerous inhibitors. A number of publications have focused on the close correspondence between thermolysin and various other zinc enzymes in the location and function of the mechanistically important groups (Argos et al., 1978, 1981; Kester & Matthews, 1977b). The above considerations make thermolysin a good model enzyme for mechanistic studies of zinc peptidases in general.

The preceding paper by Monzingo and Matthews reports the crystal structure of thermolysin complexed with *N*-(1-carboxy-3-phenylpropyl)-L-leucyl-L-tryptophan (hereafter CLT, Figure 1). This inhibitor ($K_i = 5 \times 10^{-8}$ M, Maycock et al., 1981) was designed by the same principles that afforded potent inhibitors (Patchett et al., 1980) of another zinc peptidase, the angiotensin converting enzyme (ACE). An example of one such inhibitor is MK-422 ($IC_{50} = 1.2 \times 10^{-9}$ M), the active form of the prodrug MK-421 (Figure 1) presently undergoing clinical trials as a treatment for human hypertension. The boxed portions of these inhibitors indicate the design carry-over for binding to the zinc and S_1[2] subsites. The alterations in the dipeptide fragment reflect the specificity differences between the enzymes in the S_1' and S_2' subsites.

The surprising discovery (Monzingo & Matthews, 1984) that the zinc-binding carboxyl group of CLT coordinates in a bidentate fashion, together with the availability of refined high-resolution crystallographic data for this and other TLN–inhibitor complexes, stimulated us to reinvestigate[3] the mechanism of peptide cleavage by thermolysin. In addition, we expected that such a study would be useful to us in our ongoing efforts to design new zinc endopeptidase inhibitors.

The present study adds a number of new insights to the mechanism previously proposed (Holmes & Matthews, 1981; Kester & Matthews, 1977a) and provides a rationalization for published substrate data (Morihara & Tsuzuki, 1970). We have further endeavored to explain the potency of CLT by comparing its binding mode with that of the tetrahedral in-

† From Merck Sharp & Dohme Research Laboratories, Rahway, New Jersey 07065 (D.G.H.), and the Institute of Molecular Biology and the Department of Physics, University of Oregon, Eugene, Oregon 97403 (A.F.M. and B.W.M.). *Received September 12, 1983; revised manuscript received March 30, 1984.* This work was supported in part (A.F.M. and B.W.M.) by grants from the National Science Foundation (PCM 8014311), the National Institutes of Health (GM20066), and the M. J. Murdock Charitable Trust.

[1] Abbreviations: TLN, thermolysin; CLT, *N*-(1-carboxy-3-phenylpropyl)-L-leucyl-L-tryptophan; ACE, angiotensin converting enzyme (kininase II, dipeptidyl carboxypeptidase, EC 3.4.15.1); Z, benzyloxycarbonyl; β-PPP, (β-phenylpropionyl)-L-phenylalanine. All amino acid residues have the L configuration unless specified otherwise.

[2] The nomenclature used for the amino acid residues (P) of the substrate and to name the subsites (S) of the active site is that of Schechter & Berger (1967).

[3] For a previous investigation with physical models and unrefined coordinates, see Kester & Matthews (1977a). For a further refined mechanism, see Holmes & Matthews (1981).

0006-2960/84/0423-5730$01.50/0

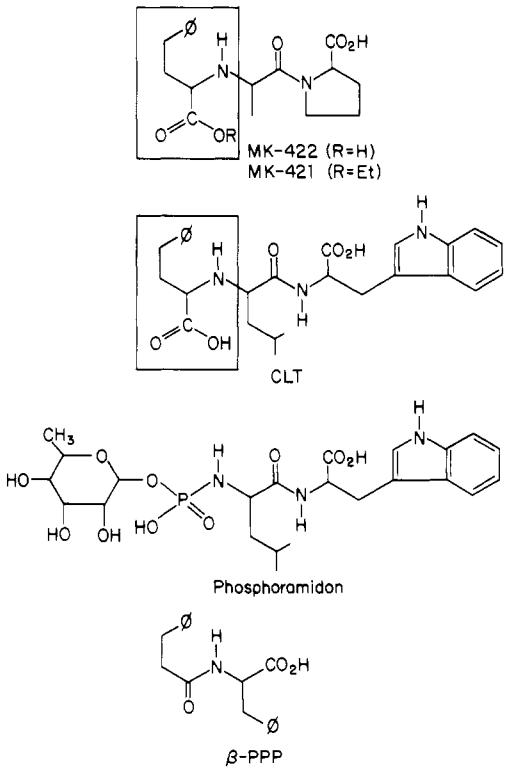

FIGURE 1: Comparison of the thermolysin inhibitor CLT with ACE inhibitor MK-422 and two other thermolysin inhibitors, phosphoramidon and β-PPP.

termediate involved in peptide cleavage.

Experimental Procedures

The interactive computer graphics studies were carried out on an Evans and Sutherland multipicture system with a color display backed by a VAX 11/780 computer.

The coordinates for native thermolysin refined to 1.6 Å (Holmes & Matthews, 1982), the CLT–TLN complex refined to 1.9 Å (Monzingo & Matthews, 1984), and the phosphoramidon–TLN complex refined to 1.9 Å (Weaver et al., 1977; A. F. Monzingo, D. E. Tronrud, and B. W. Matthews, unpublished results) were examined in the course of this study. The active sites in these two inhibitor complexes and the native enzyme were found to be essentially identical. The enzyme coordinates from the CLT–TLN complex were used in the subsequent modeling studies.

In deciding on a model substrate to study, we wanted to utilize as much crystallographic data as possible. The availability of refined coordinates for bound CLT and phosphoramidon (Figure 1), another potent inhibitor ($K_i = 2.8 \times 10^{-8}$ M) of thermolysin, suggested the use of Phe-Leu-Trp for the P_1–P_1'–P_2' sequence. Pertinent crystallographic data were not available for position P_2; consequently, a Z-Phe residue was chosen by considering substrate data (Morihara & Tsuzuki, 1970). An excerpt of these data, upon which the choice was made, is given in Table I. Phenylalanine contains all of the structural components of glycine and alanine and is the most sterically demanding residue of the variable P_2 series. Consequently, information regarding glycine or alanine substitutions can be obtained by studying a model substrate with Phe at position P_2 and ignoring the appropriate atoms. The model substrate Z-Phe-Phe-Leu-Trp can fill the active site, and further extensions of the substrate have a less dramatic effect on the reaction kinetics (Morihara & Tsuzuki, 1970).

For construction of the model substrate and tetrahedral intermediate, a Molecular Editor computer program developed by Fluder and Smith[4] was utilized. The Leu-Trp portions of the model structures were constructed from the corresponding crystallographic coordinates for complexed CLT. The remaining portions of these structures were built by using bond angles of 109.5° and 120.0° for tetrahedral and trigonal atoms, respectively. The bond lengths used are 1.54 Å for $C(sp^3)$–$C(sp^3)$, 1.51 Å for $C(sp^3)$–C(phenyl), 1.52 Å for $C(sp^3)$–C(=O), 1.47 Å for $C(sp^3)$–$N(sp^3)$, 1.43 Å for $C(sp^3)$–O(–H,R), 1.32 Å for C(=O)–N(amide or urethane), 1.24 Å for C(–N)=O (amide or urethane), 1.37 Å for C(=O)–O(urethane), 1.40 Å for C(phenyl)–C(phenyl), and 1.46 Å for $C(sp^3)$–N(amide or urethane).

A modified (Bush, 1984) version of FRODO (Jones, 1978), a computer program originally designed for use in protein crystallography, was utilized to study TLN–ligand interactions. One modification, CLARIFI (Bush, 1984), visually indicates the approximate magnitude of the interatomic interactions (attractive and repulsive) in real time as one moves all or part of the displayed structure. These interactions are approximated by a modified Lennard–Jones (6–12) function. The number of attractive and repulsive interactions are listed on a monitor while their magnitude and identities are indicated qualitatively on the display by color-coded lines. Consequently, CLARIFI allows one to be confident that close contacts (intra- or intermolecular) will not be overlooked. The display also indicates the direction of rotation about a specific bond that will minimize steric repulsions. This capability was augmented by measuring specific interatomic distances (via FRODO) and comparing them to the appropriate van der Waals radii (Fersht, 1977).

In this way we were able to rapidly obtain a qualitative estimate of the binding ability for numerous complexes resulting from translations, rotations, and dihedral angle changes of the model substrate within the active site. FRODO was also used to superimpose portions of small molecules or compare the relative positioning of two or more molecules in the active site.

Further details of the molecular modeling system, modeling strategy, assumptions, and methods used in this study are included in a separate publication (Gund et al., 1984).

Results

Michaelis Complex. In order to investigate Michaelis complexes involving coordination of the scissile peptide oxygen to zinc, we used the published coordinates for the (β-phenylpropionyl)-L-phenylalanine (β-PPP, Figure 1)–TLN complex (Kester & Matthews, 1977a) as a guide in docking our model substrate Z-Phe-Phe-Leu-Trp. Accordingly, the scissile peptide linkage (-Phe↓Leu-) was superimposed upon the zinc-coordinating amide of β-PPP. Holding the scissile peptide fixed, the -Leu-Trp portion was then superimposed upon the -Leu-Trp of phosphoramidon. Subsequently, the side chain of the P_1 Phe was moved into a position close to that of the corresponding groups in inhibitors CLT and β-PPP. Finally, the P_2 Z-Phe was fitted to the S_2 subsite such that two hydrogen bonds to the protein backbone of Trp-115 were formed as proposed by Kester & Matthews (1977a). A stereo representation of the resulting Michaelis complex is shown in Figure 2.

The P_1' and P_2' residues fit well in the active site, as expected, since they coincide with the Leu-Trp of phosphoramidon. The use of β-PPP coordinates for positioning the

[4] Drs. E. Fluder and G. Smith, Department of Scientific Information, Merck Sharp & Dohme Research Laboratories, unpublished results.

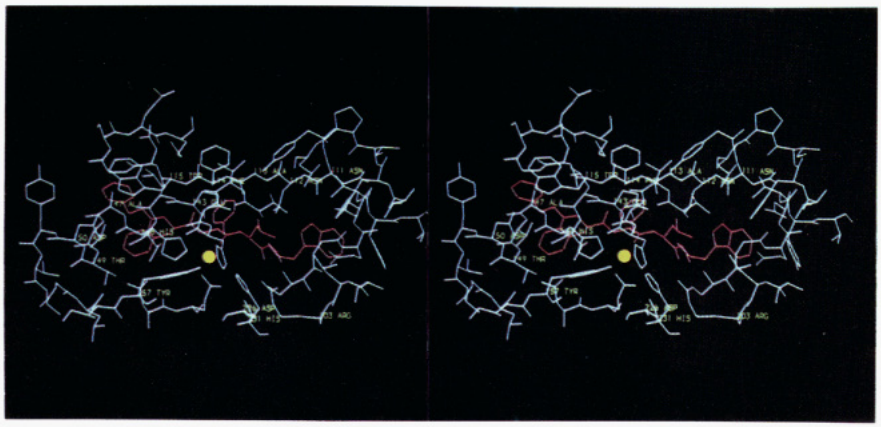

FIGURE 2: Stereo representation of the Michaelis complex involving direct coordination of the model substrate Z-Phe-Phe-Leu-Trp (red) to zinc (yellow). The active site is in white and the residue labels are green. The coordinates for the substrate in Figures 2–6 are appended to the refined thermolysin–CLT coordinate list deposited in the Brookhaven Data Bank (Monzingo & Matthews, 1984).

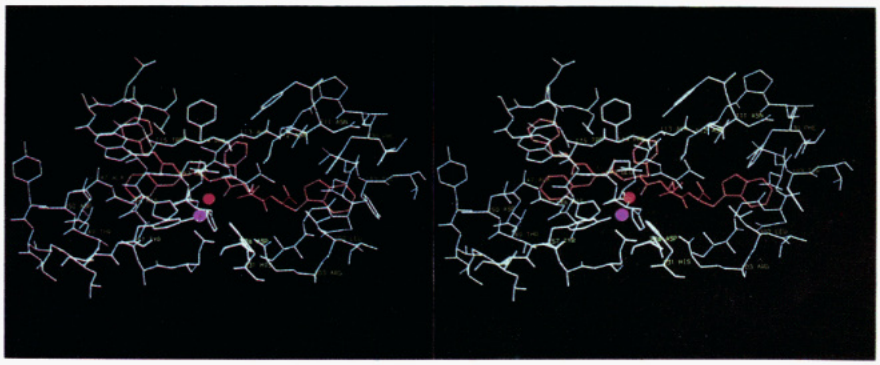

FIGURE 3: Stereo representation of the Michaelis complex *not* involving direct coordination of the model substrate to zinc (purple). The zinc-bound water molecule is represented as an orange ball.

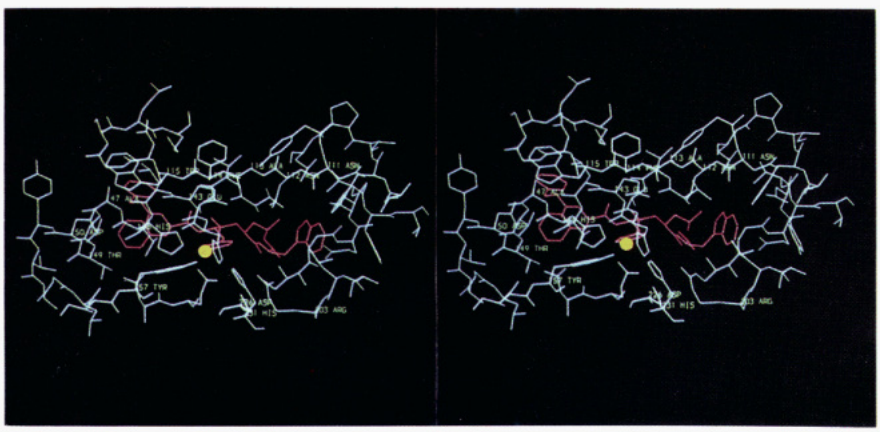

FIGURE 4: Stereo representation of the first potential tetrahedral intermediate (red). The positioning was guided by the coordinates for phosphoramidon.

scissile peptide results in the same distorted tetrahedral geometry of the zinc ligands. The P_1 Phe is positioned to bind with the Phe-114 side chain analogous to the inhibitors CLT and β-PPP. The P_2 Phe is in a reasonable position to form two hydrogen bonds with the Trp-115 backbone (2.9[5] and 2.7 Å to Trp-115 N-H and C=O, respectively). However, the P_2 Phe side chain is in steric interference with the bottom of the active-site cleft. The positioning of its benzylic methylene results in a steric repulsion with the side chain of His-146 (one of the protein zinc ligands) with some C–C distances as close as 2.1 Å. An upward movement of this side chain on the order of 1.2 Å would be required to relieve the steric interference. A displacement of this magnitude could not be achieved without considerable lengthening of the zinc–scissile peptide oxygen distance and/or extensive bond angle distortions. The same interaction would also apply to substrates with an alanine residue at P_2. Positioning of the P_2 Phe such that the side chain is not located directly over the bottom of the cleft also results in undesirable interactions. Consequently, a Michaelis complex involving coordination of the scissile peptide to the zinc appears unlikely for substrates with a residue of L configuration at P_2.

We then proceeded to investigate alternative Michaelis complexes, where the scissile peptide oxygen is not coordinated to the zinc. It is known that the hydrophobic pocket at the S_1' subsite has a major effect on the specificity of this enzyme

[5] Heteroatom distance.

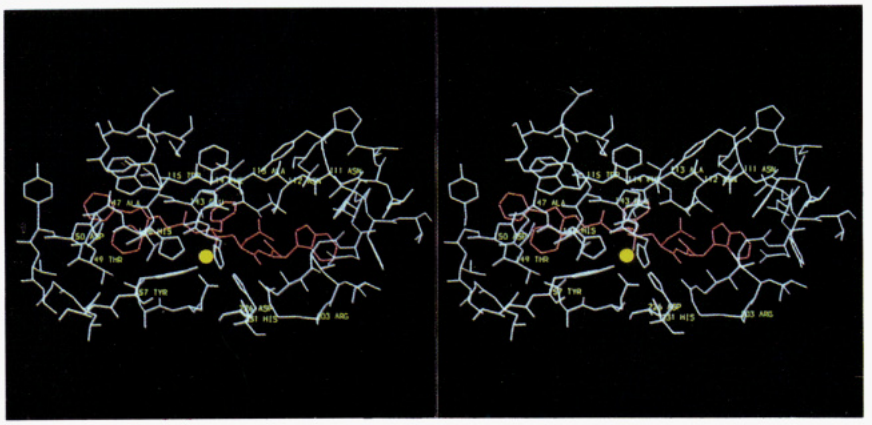

FIGURE 5: Stereo representation of the second potential tetrahedral intermediate. The hydrated scissile peptide is coordinating to zinc (yellow) in a bidentate fashion.

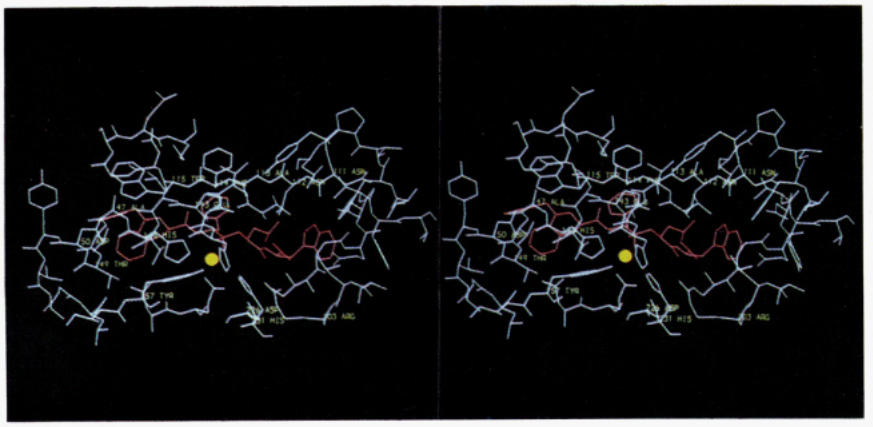

FIGURE 6: Stereo representation of the third potential tetrahedral intermediate. The hydrated scissile peptide is positioned such that one of its oxygens is a zinc ligand and the other is hydrogen bonding to His-231 and Tyr-157.

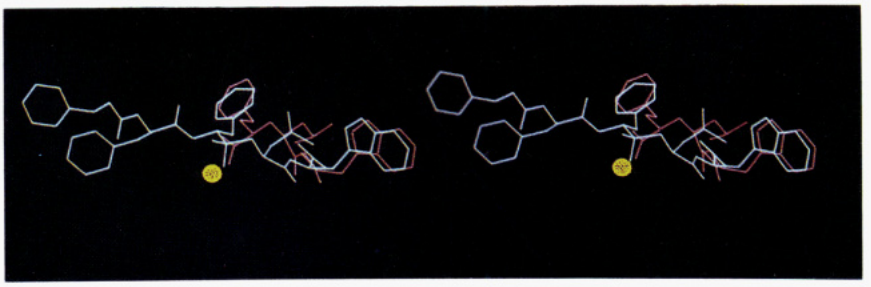

FIGURE 7: Stereo representation showing the relative positioning of bound CLT (red) and the preferred (second) tetrahedral intermediate (white) orientation. To enhance clarity, only the zinc (yellow) from the active site is shown.

(Matsubara et al., 1965, 1966; Morihara & Tsuzuki, 1970). Therefore, we assumed that the substrate would interact strongly with this pocket in the Michaelis complex. The substrate data shown in Table I also indicated that the P_2, P_1', and P_2' side chains can interact with the enzyme in the Michaelis complex. Upon investigation of various plausible complexes it was found that the Michaelis complex shown in Figure 3 fulfilled most of our requirements. A direct coordination of the scissile peptide to the zinc is not involved, and the P_2, P_1', and P_2' side chains are interacting with the active site without forcing any bad contacts. The scissile peptide oxygen is positioned 4.2 Å above the zinc and within hydrogen-bonding distance of the zinc-coordinating water molecule (2.7 Å) as well as the N^{ϵ} of His-231 (2.7 Å). The P_2 Phe is positioned such that its side chain is binding with the Tyr-157 side chain (vide infra). The P_1' Leu is largely, but not completely, immersed in the S_1' hydrophobic pocket and pointing toward the bottom of this pocket. A small rotation of the Asn-112 side chain about the C_α–C_β bond[6] may position the side-chain oxygen within hydrogen-bonding distance of both the scissile peptide nitrogen (2.7 Å) and the P_2' Trp peptide nitrogen (3.1 Å). Furthermore, the P_2' Trp carboxyl group is then able to hydrogen bond with the Asn-112 side-chain nitrogen (3.0 Å). The P_2' Trp side chain is positioned over a hydrophobic patch formed by Phe-130, Tyr-193, and Leu-202.

In the Michaelis complex shown in Figure 3, the P_1 Phe side chain is not in a position to interact strongly with the active site. This side chain can be repositioned to bind with the Phe-114 side chain by a rotation about the P_1 Phe C_α–scissile peptide bond. However, in doing so, we also rotate the P_2 Phe

[6] The conformation of this side chain is the most significant difference between the active sites of the native enzyme and the CLT–TLN complex. The conformation shown in Figure 3 corresponds to that of the CLT–TLN complex.

residue out of the active-site cleft. Consequently, we cannot simultaneously obtain favorable interactions with the active site through both the P_1 and P_2 side chains in the presently considered Michaelis complexes. In fact, the substrate data (Table I) do not support a *simultaneous* interaction of these two side chains with the enzyme. The systematic changes in the P_2 residue were carried out on substrates containing a glycine at P_1, avoiding the opportunity for binding to the Phe-114 side chain. The variable P_1 data involve substrates lacking a suitable residue at position P_2 for interacting with the Tyr-157 side chain. The relationship of these two possible Michaelis complexes to the substrate data is discussed in more detail later.

Tetrahedral Intermediate Complex. The model substrate Z-Phe-Phe-Leu-Trp was converted to the corresponding tetrahedral intermediate formed by the addition of water to the scissile peptide. Three alternate binding orientations of this tetrahedral intermediate to the active site were investigated.

The first orientation utilizes the refined coordinates of complexed phosphoramidon for positioning in the active site. An *N*-phosphoryl group is a good mimic of a hydrated peptide. The P–O bonds are only slightly longer than the corresponding C–O bonds, and both the *N*-phosphoryl group and a hydrated peptide are tetrahedral. Phosphoramidon complexes to thermolysin with one of its *N*-phosphoryl oxygens hydrogen bonding to Glu-143 and another as a zinc ligand. In orientating the tetrahedral intermediate, the hydrated peptide was superimposed, as closely as possible, upon the corresponding atoms of the *N*-phosphoryl group. Consenquently, the negatively charged oxygen was positioned 2.0 Å from the zinc, resulting in a distorted tetrahedral zinc complex. The OH group can hydrogen bond with the carboxyl of Glu-143 with a heteroatom distance of 2.5 Å. With the hydrated peptide held fixed, the Leu-Trp portion was superimposed upon the Leu-Trp of phosphoramidon. Finally, the P_1 Phe and P_2 Z-Phe were fitted to the S_1 and S_2 subsites while an attempt was made to form two hydrogen bonds to Trp-115 as previously proposed (Kester & Matthews, 1977a). The resulting complex is illustrated in Figure 4.

As shown, a very poor fit at the S_1 subsite was obtained. The side chain of the P_1 Phe is 8.7 Å from the side chain of Phe-114, much too far for hydrophobic binding to occur. Also, the P_1 Phe side chain has a number of bad contacts with the opposite side of the cleft. Attempts to move this side chain closer to Phe-114 by rotating about the bond to the cleaving peptide resulted in a loss of the hydrogen bonds with Trp-115. Even in the orientation shown in Figure 4, the P_2 Phe oxygen is 3.3 Å from the Trp-115 nitrogen and the P_2 Phe nitrogen is 2.9 Å from the Trp-115 oxygen. A poor fit is also obtained at the S_2 subsite. The P_2 Phe side chain is approximately 0.8 Å too close to the His-146 side chain on the bottom of the cleft (closest C–C distance 2.5 Å). Efforts to obtain a good fit by ignoring the coordinates for phosphoramidon, but still requiring that one of the oxygens of the hydrated peptide coordinates to zinc (at ca. 2.0 Å) and the OH group hydrogen bonds to the carboxyl of Glu-143, were also unsuccessful.

The second orientation was inspired in part by the recent results of Monzingo & Matthews (1984) wherein the zinc-binding carboxyl of CLT coordinates to the zinc in a bidentate fashion. The coordinates for this carboxyl were utilized for the initial positioning of the tetrahedral intermediate. The hydrated peptide oxygens and carbon atom were superimposed, as closely as possible, upon this carboxyl group. The Leu-Trp portion was positioned by utilizing the corresponding coordinates for phosphoramidon and then further adjusted for maximal harmony with the S_1' and S_2' subsites. Subsequently, the P_1 Phe and P_2 Z-Phe were fitted to the S_1 and S_2 subsites, forming two hydrogen bonds to Trp-115 and hydrophobic interactions with Phe-114 and the bottom of the cleft. Finally, small adjustments in the positioning of the tetrahedral intermediate were made to improve the fit. These adjustments displaced the hydrated peptide somewhat (ca. 0.3 Å) from the positioning of the zinc-binding carboxyl of CLT. The resulting complex is illustrated in Figure 5.

As shown, a much improved fit over the first orientation was obtained. The two hydrogen bonds with Trp-115 can now be formed simultaneously with hydrophobic binding at Phe-114 in the S_1 subsite. The P_1 phenyl group is 4.1 Å from the Phe-114 phenyl group, in very close agreement with the corresponding distance found for CLT and β-PPP. The P_2 Phe oxygen is 2.8 Å from the Trp-115 nitrogen and positioned such that a nearly linear hydrogen bond is formed. The nitrogen of the P_2 Phe is 2.7 Å from the Trp-115 oxygen and also positioned for a nearly linear hydrogen bond. The fit of the P_2 Phe side chain in the S_2 subsite has also been improved somewhat. The closest C–C distance has been lengthened from 2.5 to 2.8 Å. It should also be noted that in this orientation, as well as in the first and following orientations, the P_2 Phe phenyl group is positioned too close to the Asp-150 side-chain carboxyl group (closest contact 2.0 Å). Consequently, a movement of the Asp-150 side chain may be necessary to accommodate the phenyl group. The Asp-150 carboxyl group is within hydrogen-bonding distance (3.0 Å) of the indole N-H of Trp-115. Therefore, one would expect a rotation of the Asp-150 side chain to carry an energy penalty with it. A portion of the P_2 Phe phenyl group is located 6.0 Å above the bottom of an indentation in the cleft floor formed by Thr-149. The oxygens of the hydrated peptide are both positioned at 2.1 Å from the zinc, resulting in a pentacoordinate complex. One of these oxygens may also hydrogen bond to the N^{ϵ}-H of His-231 (2.9 Å)[5] and the O-H of Tyr-157 (2.6 Å).[5] The other is within hydrogen-bonding distance of one of the carboxyl oxygens of Glu-143 (2.8 Å). The equidistant positioning of the hydrated peptide oxygens on the zinc results in some crowding with the enzyme zinc ligands. Perhaps a minor adjustment of these ligands and/or a slight lengthening of one of the substrate oxygen–zinc distances may occur to prevent this crowding. In fact, one of the CLT oxygen–zinc distances was observed to be somewhat longer than the other (Monzingo & Matthews, 1984). The nitrogen of the hydrated peptide is 3.2 Å from the other Glu-143 carboxyl oxygen and 4.0 Å from the N^{ϵ} of His-231.

In the third orientation, one of the hydrated peptide oxygens was positioned as a zinc ligand (2.0 Å) and the other such that hydrogen bonds with the N^{ϵ}-H of His-231 (2.7 Å)[5] and the O-H of Tyr-157 (2.7 Å)[5] are possible. While these interactions were being maintained, an attempt was made to maximize the fit of the tetrahedral intermediate in the active site. The resulting complex is illustrated in Figure 6.

Upon casual inspection, the fit appears to be reasonable. However, a more rigorous examination reveals some negative interactions. The hydrated peptide nitrogen and the C_α of P_1 Phe are positioned closer to the Glu-143 side of the cleft than in the previous two orientations. As a result, the two halves of the tetrahedral intermediate on either side of the scissile peptide are also pressed closer to this side of the cleft. A number of adjustments to the conformation of the two halves were made to minimize bad contacts. Even so, the P_1' Leu side chain comes within 2.4 Å (C–O distance) of the Glu-143 carboxyl and engages in an intramolecular C–C contact of 2.5 Å. The P_1 Phe phenyl group has been moved 0.7 Å closer to Phe-114 than the distance found for CLT, β-PPP, and the

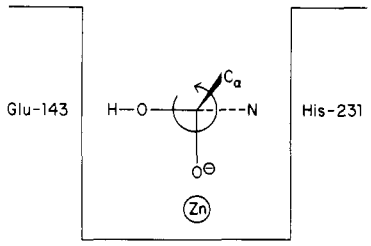

FIGURE 8: Movement of the hydrated scissile peptide within the active site as one proceeds from the first tetrahedral intermediate orientation to the third.

second orientation. Furthermore, the P_2 Phe side chain is again within 2.5 Å of the His-146 side chain on the bottom of the cleft.

Discussion

Comparison of Tetrahedral Intermediate Orientations. The three tetrahedral intermediate orientations basically relate to each other by a rotation[7] of the hydrated peptide as indicated in Figure 8. In the first orientation the hydrated peptide oxygens are pointed toward Glu-143 and the zinc. In order to attain the second orientation, the hydrated peptide must be rotated until the oxygens are straddling the zinc at the bottom of the cleft. Finally, the third orientation is obtained by continuing to rotate in the same direction until one of the oxygens points toward the His-231 side of the cleft and the other toward the zinc. While undergoing the rotation, the hydrated peptide nitrogen and the C_α atom of P_1 Phe are moving toward the opposite side of the cleft (Figure 8).

From these studies it appears that the second orientation situates the hydrated peptide nitrogen and the C_α atom such that the attached halves of the model substrate are optimally placed relative to the sides of the cleft. The first orientation positions these atoms too far from the Glu-143 side. When one moves the hydrated peptide nitrogen and attached Leu-Trp close enough for positive interactions, as was done in Figure 4, the P_1 and P_2 residues are further displaced from the Glu-143 side. At the other extreme, the third orientation positions these atoms too close to the Glu-143 side.

All of these orientations involve a steric interaction of the P_2 Phe side chain with the bottom of the cleft [although not to the extent of the first Michaelis complex (Figure 2)]. Nevertheless, this interaction is improved in the second orientation. The closest C–C distance is still about 0.5 Å too close, but one must be cognizant that the protein and inhibitor coordinates, upon which this study is based, each have uncertainties of about 0.2 Å. Also, the positioning of the P_1–P_1'–P_2' residues was guided by coordinates for inhibitors where a compromise due to interactions of a P_2 residue was not required. Furthermore, small distortions about a number of contiguous bond angles [with a modest energy penalty (Fersht, 1977)] to relieve this interaction may be more than compensated for by improved binding to the active site. Finally, minor displacements of the protein backbone and side chains in the active site (perhaps due to small differences between the crystal and solution structures) provide an additional means of accommodating this apparent moderate steric interference.

The assertion that the tetrahedral intermediate binds to zinc in a bidentate fashion is given further credence by the finding that the carboxyl of CLT coordinates bidentate. The coordinates for the carboxyl oxygens are close to those of the hydrated peptide oxygens in the second orientation (vide infra). Furthermore, inhibitors containing hydroxamic acid groups bind to zinc in a bidentate fashion via the two oxygens while also hydrogen bonding to Glu-143 and His-231 (Holmes & Matthews, 1981). In the second orientation, the hydrated peptide oxygens are modeled exactly equidistant from the zinc. However, as mentioned earlier, a slight lengthening of the oxygen–zinc distance for the hydrated peptide oxygen closest to Glu-143 would relieve some crowding of the zinc ligands. This adjustment would also result in a bidentate coordination in closer analogy to the CLT–thermolysin complex. Subsequent to this computer graphics study, a rotation of the type depicted in Figure 8 was found in comparing the complexes of TLN with phosphoramidon and *N*-phosphoryl-L-leucine amide (A. F. Monzingo, D. E. Tronrud, and B. W. Matthews, unpublished results). The *N*-phosphoryl group was found in a position that is related to that of phosphoramidon by a 25° rotation toward a bidentate orientation. In view of these modeling results, the available experimental data, and the fact that we are able to rationalize the substrate data (vide infra), we propose that the second tetrahedral intermediate orientation (Figure 5) is a reasonable approximation of the transition state (Hammond, 1955) for analogous substrates.

Table I: Selected Thermolysin Substrate Data Illustrating the Effect of Side-Chain Variations at Positions P_2, P_1, P_1', and P_2'[a]

Peptide P_2–P_1–P_1'–P_2'	K_M(mM)	k_{cat}(sec.$^{-1}$)	k_{cat}/K_M(sec.$^{-1}$ mM^{-1})
Z-Gly-Gly-Leu-Ala	12.2	362	30
Z-Ala-Gly-Leu-Ala	8.6	5,208	606
Z-Phe-Gly-Leu-Ala	0.9	446	491
Z-Gly-Leu-Ala	10.6	781	78
Z-Ala-Leu-Ala	4.9	997	203
Z-Phe-Leu-Ala	0.6	398	678
Z-Phe-Gly-Ala	7.4	8	1
Z-Phe-Ala-Ala	2.6	22	8
Z-Phe-Leu-Ala	0.72	416	578
Z-Phe-Phe-Ala	0.45	162	360
Z-Phe-Tyr-Ala	0.72	7	10
Z-Gly-Leu-Gly	10.8	65	6
Z-Gly-Leu-Ala	10.6	781	78
Z-Gly-Leu-Leu	2.6	374	144

[a] Morihara & Tsuzuki, 1970.

Rationalization of Substrate Data. Morihara & Tsuzuki (1970) reported that the substrates listed in Table I followed Michaelis–Menten kinetics. Consequently, we made the assumption that their reported K_M values are equal to the corresponding K_s values. This assumption is supported by the finding that the K_M approximates the K_s for a similar thermolysin substrate (Morgan & Fruton, 1978). The thermodynamic relationship between the standard-state Gibbs energy change and the association constant K (or $1/K_s$) given by the equation $\Delta G = -RT \ln K$ was used to calculate the ΔG_b[8] for formation of the Michaelis complex from the free enzyme and substrate (Fersht, 1977; Page, 1980). The relationship $k_{cat}/K_M = kT/h \exp[-\Delta G^*/(RT)]$, derived from transition-state theory, was used to calculate the standard-state Gibbs energy of activation (ΔG^*)[8] relative to the free enzyme and substrate (Fersht, 1977; Page, 1980). These calculated standard-state

[7] The distance to the zinc was maintained at ca. 2.0 Å, and other small adjustments were also made.

[8] At a standard state of 1 M, 40 °C, and pH 7.0. The K_M, k_{cat}, and k_{cat}/K_M values reported in Table I were measured at 40 °C and pH 7.0.

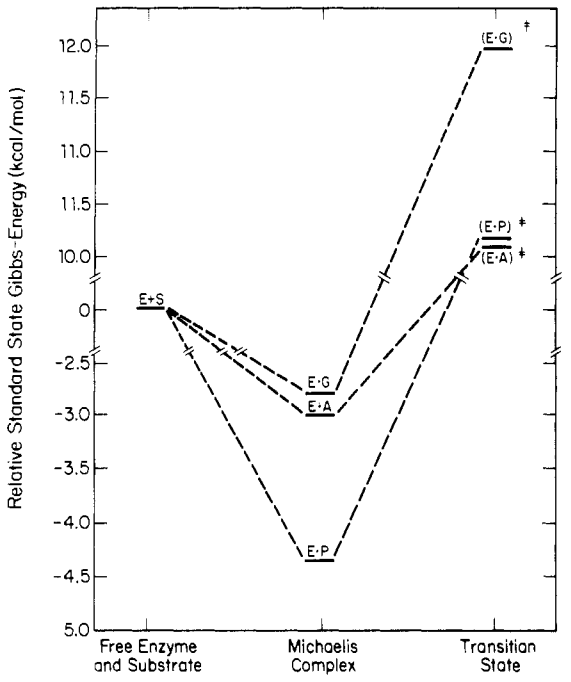

FIGURE 9: Reaction-coordinate diagram illustrating the standard-state Gibbs energy changes for the conversion of thermolysin (E) and the variable P_2 substrates (S) listed in Table I to the Michaelis complex and then the transition state. The substrates Z-Gly-Gly-Leu-Ala, Z-Ala-Gly-Leu-Ala, and Z-Phe-Gly-Leu-Ala are represented by G, A, and P, respectively. The Gibbs energies given are relative to free enzyme and substrate and at a standard state of 1 M, 40 °C, and pH 7.

Gibbs energy changes for the substrates with a variable P_2 are illustrated in the reaction-coordinate diagram of Figure 9 (Jencks, 1980; Page, 1980).

P_2 Position. As shown in Figure 9, substitution of an alanine for glycine at P_2 has a very small effect on the stability of the Michaelis complex ($\Delta\Delta G_b$ = –0.22 kcal/mol). This indicates either that the alanine methyl group is not positioned to interact with the enzyme or that its positive interactions are counterbalanced by unfavorable energy changes. The positioning of the P_2 Phe side chain methylene in our proposed Michaelis complex (Figure 3) makes the latter possibility seem plausible. This methylene is adjacent to the hydroxyl end of the Tyr-157 side chain. A P_2 alanine may position its methyl group analogously. The net result may be that the hydrophobic binding gained with the nearby hydrocarbon region of Tyr-157 is negated by desolvation of the hydroxyl group and an entropy loss in the P_1–P_2 region of the substrate associated with placing a side chain in the mouth of the cleft. Even though this energy balance would be "invisible" in the measured K_M, it may still serve a useful purpose. Specifically, some of the entropy loss and desolvation that are required to achieve the transition state has already been accomplished (and paid for) in the Michaelis complex (Jencks, 1980; Lipscomb, 1982).

Substitution of a phenylalanine for glycine at P_2 lowers the Gibbs energy of the Michaelis complex by 1.63 kcal/mol. Consequently, an overall favorable interaction of this side chain with the enzyme seems assured. The side-chain methylene probably does not affect the observed binding appreciably since its contribution may be negated in the same way as the alanine methyl group. However, the side-chain phenyl group may provide the additional observed binding because of its interactions with the remainder of the Tyr-157 side chain. In fact, an orthogonal arrangement for phenyl groups in proteins, analogous to that shown in Figure 3 for the P_2 Phe side chain and Tyr-157, has been suggested to be the most favorable (Thomas et al., 1982; K. A. Thomas, E. M. Fluder, and G. M. Smith, unpublished results).

The important consideration, from the standpoint of rapidly converting substrate to products, is that the Gibbs energy of the transition state be as low as possible (resulting in a higher k_{cat}/K_M). In this regard the most efficient P_2 residue of the series is alanine. The intrinsic binding energy (Jencks, 1981) of the alanine methyl group is apparently utilized to lower the transition-state Gibbs energy by 1.88 kcal/mol relative to a P_2 glycine (Figure 9). The magnitude of this stabilization is within the estimated range of intrinsic binding energy available from a methyl group (Jencks, 1981). As shown in Figure 5, the P_2 Phe side-chain methylene is positioned such that hydrophobic binding is possible. An analogously positioned alanine methyl group may stabilize the transition state by hydrophobic binding in the same way.

The $\Delta G^{\ddagger}$ values illustrated in Figure 9 indicate that the phenyl group of a P_2 Phe slightly destabilizes the transition state relative to a P_2 alanine. In our proposed transition state this phenyl group is largely positioned above an indentation in the bottom of the cleft (Figure 5). The distance from the phenyl group to the bottom of the indentation may be too long (6.0 Å) for its full binding potential to be realized. Additionally, the Asp-150 side chain may have to rotate about its C_α–C_β bond and forfeit a hydrogen bond with the Trp-115 side chain in order to accommodate the phenyl group. The net result may be that the phenyl group actually destabilizes the transition state because its binding interactions with the bottom and sides of the cleft are slightly outweighted by a necessary rotation of the Asp-150 side chain.

According to transition-state theory, the k_{cat} values are determined by the relative Gibbs energies of the Michaelis complex and the transition state for each individual substrate (Page, 1980). The greater the Gibbs energy increase required to achieve the transition state from the Michaelis complex, the smaller the k_{cat}. By inspection of Figure 9 it becomes apparent that the high k_{cat} for the substrate with a P_2 alanine (k_{cat} = 5208) is due to the selective stabilization of the transition state by the alanine methyl group. In contrast, the phenyl group of a P_2 Phe selectively stabilizes the Michaelis complex and hence greatly reduces the k_{cat} (446) compared to a P_2 alanine.

In discussing the effects of a P_2 Ala or Phe side chain on the Gibbs energy of the Michaelis complex and the transition state, we have used the substrate with a P_2 glycine as our reference point. However, the lack of a side chain at P_2 makes the Michaelis complex involving a coordination of the scissile peptide to zinc (Figure 2) sterically feasible. Nevertheless, if the scissile peptide displaces the zinc-bound water molecule, as did the inhibitor β-PPP, this may be a nonproductive binding mode. As such the "apparent" K_M and k_{cat} would be equally lowered, leaving k_{cat}/K_M and our analysis of the relative transition-state stabilities unchanged (Fersht, 1977). If the apparent K_M of the substrate containing a P_2 glycine has been lowered, then the calculated Gibbs energies of the Michaelis complexes for substrates with an alanine or phenylalanine at P_2 would underestimate the binding contribution of the side chains relative to glycine but not relative to each other. Since the electrostatic environment in the zinc region is particularly suited to formation of the tetrahedral intermediate (vide infra), it seems likely that, even in the absence of a steric interaction at P_2, the scissile peptide would not coordinate to the zinc before a water molecule has begun to attack.

P_1 Position. As mentioned earlier, the data (Table I) for substrates unable to interact with the Tyr-157 side chain

suggest involvement of a Michaelis complex related to that in Figure 3 by a rotation about the P_1 C_α–scissile peptide bond. In this way the P_1 side chain becomes positioned adjacent to the Phe-114 side chain. Consequently, one would expect the more hydrophobic P_1 side chains to decrease the K_M as is indeed observed (Table I). When the proposed transition state is reached (Figure 5), the P_1 side chain is again adjacent to the Phe-114 side chain. Therefore, one would expect the transition state to be increasingly stabilized (resulting in higher k_{cat}/K_M values) by the more hydrophobic P_1 side chains. As shown in Table I, this is again in agreement with experiment.

When a substrate is able to interact with either Phe-114 or Tyr-157, one would expect the relative strengths of these interactions to determine the ratio of the two possible Michaelis complexes. A prediction which follows from the two Michaelis complex proposal is that the effect of the P_1 and P_2 side chains on the stability of the Michaelis complex will not be additive. However, some enhancement in binding resulting from the second side chain may be possible due to minor interactions with the enzyme and an increase in entropy associated with the population of another Michaelis complex. Since similar transition states appear to be involved, a Michaelis complex wherein hydrophobic binding with Phe-114 occurs would require a rotation about the P_1 C_α–scissile peptide bond back to the conformation shown for the substrate in Figure 3 before (or as) the transition state is approached.

P_1' Position. Comparison of the K_M values (Table I) for substrates with increasingly bulky side chains at position P_1' reveals another interesting progression. The K_M values decrease as the P_1' residue is increased in size (and hydrophobicity) from Gly to Phe, indicating improved binding in the S_1' pocket. This decrease in the Gibbs energy of the Michaelis complex reverses as we continue to increase the size of the side chain beyond phenylalanine. As mentioned earlier, substrates with a hydrophobic side chain at P_1, such as those we are presently considering, will probably form a Michaelis complex related to that in Figure 3 by a bond rotation within the P_1 residue. This conformational change would not be expected to greatly change the positioning of the P_1' and P_2' residues. Consequently, for our present comparison of the P_1' side chains we will refer to the Michaelis complex shown in Figure 3. An inspection of this complex shows the P_1' side chain pointing toward the bottom of the S_1' pocket. An analogous docking of similar model substrates with a P_1' Phe or Tyr indicated that a Phe is well accommodated by the pocket but larger residues (especially a Trp) may result in steric interference with the bottom of the pocket. Consequently, one would expect increasingly stabilized Michaelis complexes (lower K_M's) as one proceeds from Gly to Phe, in agreement with experiment. Further lengthening of the side chain may result in a displacement of the substrate from the proposed Michaelis complex due to a steric interaction with the bottom of the pocket. Substitution of a Tyr at P_1' increases the K_M slightly relative to P_1' Phe (Table I), and a similar substrate with Trp at P_1' was not hydrolyzed by the enzyme (Morihara & Tsuzuki, 1970).

A comparison of the Michaelis complex (Figure 3) with the tetrahedral intermediate (Figure 5) shows that the P_1' Leu side chain has undergone a conformational change about the C_α–C_β bond. In the tetrahedral intermediate this side chain is pointing toward the side of the S_1' pocket rather than the bottom. When a tyrosine is substituted for the P_1' Leu and oriented in the S_1' pocket analogously, some steric interactions are encountered with the side of the pocket. The phenolic oxygen is within 2.5 Å of the Leu-133 and Phe-130 side chains. Furthermore, the required conformational change within the limited space of the S_1' pocket may be more difficult for the larger side chains. These observations may account for the lowering of k_{cat} (and k_{cat}/K_M) as the P_1' side chain increases in size beyond Leu. A report by Pank et al. (1982), wherein a correlation between the P_1' side-chain hydrophobicity constant π_R and k_{cat}/K_M for thermolysin substrates was shown to break down for the longer side chains, also supports the present modeling results.

P_2' Position. For the final residue position to be considered, P_2', the relevant substrate data are listed in Table I. In the proposed Michaelis complex (Figure 3) the P_2' Trp side chain is interacting with a hydrophobic patch (formed by Phe-130, Tyr-193, and Leu-202) on the bottom and end of the active-site cleft. In modeling an alanine at position P_2', we oriented the methyl group analogously to the P_2' side-chain methylene in Figure 3. As such, the penetration of the P_1' Leu side chain into the hydrophobic pocket may be limited in order to avoid a steric interaction with the hydrophobic patch. Consequently, even though the alanine methyl group can bind with the hydrophobic patch, this stabilization of the Michaelis complex may be negated by less binding in the S_1' pocket relative to that achieved when P_2' is occupied by glycine. This energy balance may explain the comparable K_M values for the substrates with a glycine or alanine at P_2'. Once the transition state is reached and full penetration into the S_1' pocket has been attained, differential binding in the S_1' pocket may no longer be a factor. Consequently, the enhanced binding available from the alanine methyl group can now be expressed (i.e., k_{cat}/K_M is increased). When the P_2' residue is a leucine, the penetration of the P_1' leucine side chain into the hydrophobic pocket may be limited in the Michaelis complex analogous to the substrate with alanine at P_2'. However, the increased binding between the P_2' leucine and S_2' hydrophobic patch may be greater than the energy penalty for limited penetration into the S_1' hydrophobic pocket resulting in a lower K_M. This increased hydrophobic binding at the S_2' subsite may also be expressed in the transition state along with full penetration into the S_1' pocket resulting in the highest k_{cat}/K_M of the series.

Mechanism of Peptide Cleavage by Thermolysin. A schematic representation of the mechanism proposed herein is given in Figure 10. We propose that substrates, analogous to the model substrate, do not coordinate directly to the zinc in the Michaelis complex. A nucleation at the S_2' subsite with partial penetration into the S_1' subsite provided a rationalization for the substrate data in Table I. We further propose that the substrate completes its penetration into the active-site cleft as the tetrahedral intermediate is approached. Consequently, the steric interaction of the P_2 side chain with His-146 shown in Figure 2 is never encountered.

In the proposed Michaelis complex (Figure 3) the scissile peptide is tilted such that it can hydrogen bond to the zinc-bound water molecule and His-231. As the scissile peptide moves toward the zinc, it may become wedged between His-231, Tyr-157, and the zinc-bound water molecule. This trajectory may cause the water molecule to move along the zinc surface toward Glu-143 and become positioned for attack on the scissile peptide. In addition to functioning as a general base (Kester & Matthews, 1977a), the Glu-143 carboxyl group may also act as a proton shuttle, transferring the abstracted proton from the zinc-bound water molecule to the scissile peptide nitrogen in the tetrahedral intermediate. As shown in Figure 5, one of the Glu-143 carboxyl oxygens is 3.2 Å from the nitrogen, making a direct proton transfer plausible. This

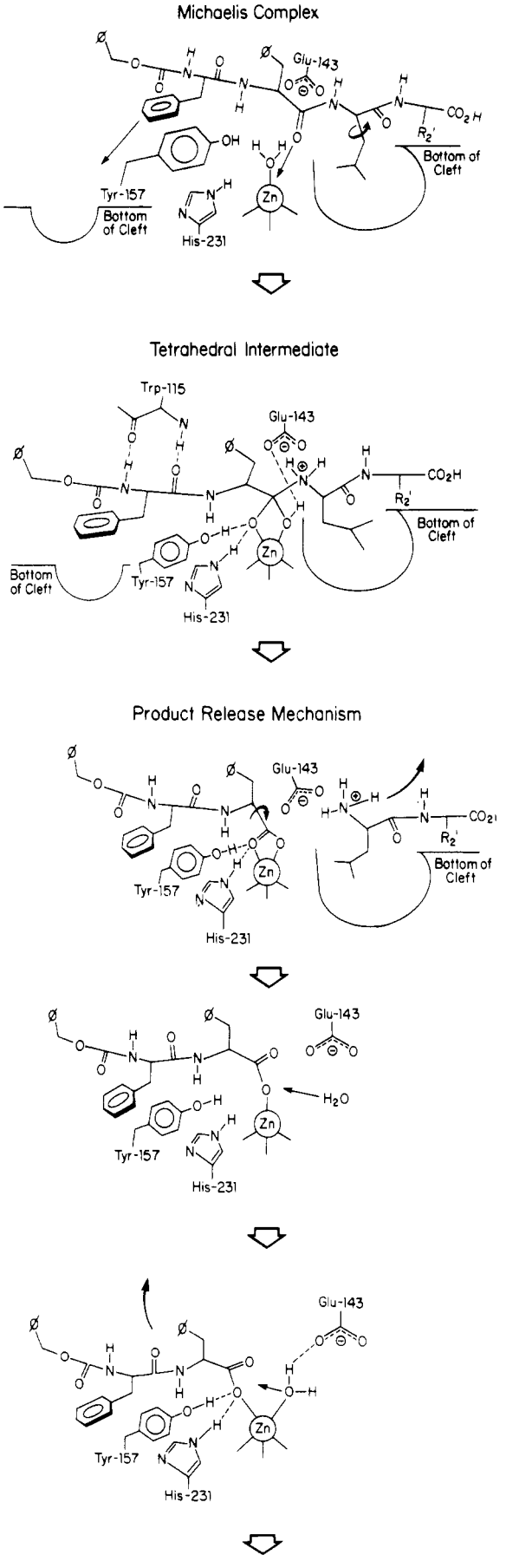

FIGURE 10: Schematic representation of the proposed mechanism for peptide cleavage by thermolysin.

dual function for the Glu-143 carboxyl group results in a "cis" addition of water across the peptide bond. Subsequently, the Glu-143 carboxyl may stabilize the tetrahedral intermediate by a salt bridge with the now positively charged nitrogen. Alternatively, it is possible that the scissile peptide nitrogen might obtain a proton from a water molecule positioned near His-231, resulting in a "trans" addition of water. However, an attempt to model a water molecule in this position indicated that some (nonhydrogen) interatomic distances as close as 2.4 Å would be encountered. Consequently, a number of changes in the tetrahedral intermediate complex (Figure 5) would be required to accommodate this water molecule. Furthermore, the Glu-143 carboxyl group would still need to lose the acquired proton in order to form a salt bridge with the protonated amine and assist in the subsequent C–N bond cleavage as described below.

The question of a cis vs. trans addition to the scissile peptide bond has also been confronted in mechanistic studies of serine proteases. The stereoelectronic theory of Deslongchamps (1977) and the principle of microscopic reversibility were invoked in proposing a mechanism wherein the cis addition of the serine hydroxyl group across the scissile peptide occurs with a necessary inversion of the leaving nitrogen before protonation (Bizzozero & Dutler, 1981). Since inversion of pyramidal nitrogen atoms is very fast (e.g., 2×10^8 s^{-1} for ammonia at 300 K), the necessary inversion in this mechanism was considered quite feasible. A more recent mechanistic study of serine proteases (Asboth & Polgar, 1983) has questioned the importance of stereoelectronic control in enzymatic reactions wherein hydrogen bonding and other interactions are involved. Following similar reasoning, we propose that water is added to the scissile peptide bond in a cis fashion, perhaps with an inversion at the leaving nitrogen before accepting a proton from Glu-143.

The Glu-143 carboxyl group may also stabilize the tetrahedral intermediate by hydrogen bonding (2.8 Å)[5] with the hydroxyl group derived from the nucleophilic water molecule. Tyr-157 and His-231 are within hydrogen-bonding distance of the hydrated peptide oxygen and may help stabilize the tetrahedral intermediate. Further stabilization of the tetrahedral intermediate may be afforded by two hydrogen bonds to the peptide backbone of Trp-115 and various other interactions mentioned earlier.

The next step of the mechanism involves cleavage of the C–N bond in the tetrahedral intermediate. The Glu-143 carboxyl group may assist this step by once again functioning as a proton shuttle. This carboxyl is positioned such that it may abstract the remaining proton on the oxygen derived from the nucleophilic water molecule and deliver it to the generated primary amine. In this way, the zinc remains neutralized throughout the reaction and the amine attains the protonation state it desires at neutral pH. This last proton transfer leaves the Glu-143 carboxyl oxygen close to an oxygen of the generated carboxyl group without the ability to hydrogen bond to it. Consequently, a repulsion may exist that triggers a rotation of the product carboxyl (Figure 10) to a monodentate orientation. This rotation would place one of the carboxyl oxygens too close to the nitrogen of the amine product and hence may "push" the amine product partially out of the active site, thereby reducing its binding affinity and facilitating its release. The Glu-143 carboxyl group is apparently positioned quite strategically by the enzyme since it may catalyze two proton transfers, help stabilize the transition state, and trigger the release of products. A nearby water molecule may now move into position as the fifth zinc ligand. The resulting

pentacoordinate zinc complex may be stabilized similarly to the tetrahedral intermediate. Departure of the carboxyl-containing cleavage product and movement of the zinc-bound water molecule to the native position completes the catalytic cycle.

The product release mechanism suggested herein is not meant to exclude the possibility that the carboxyl product may be released first. We only propose that the rate of release of the amine product is faster than that of the carboxyl product. This proposal is based upon the partial release of the amine product as the generated carboxylate group becomes a monodentate zinc ligand. Studies of the reverse reaction (i.e., peptide synthesis) catalyzed by thermolysin provide useful data pertaining to product release. The kinetic data for the thermolysin-catalyzed coupling of Z-Asp and Phe-OMe (Oyama et al., 1981) indicated that the carboxyl-containing substrate (Z-Asp) binds first, followed by the amine-containing substrate (Phe-OMe). In another study Wayne & Fruton (1983) presented kinetic data for the thermolysin-catalyzed coupling of Z-Phe with Phe-OMe and with Phe-Gly-OMe. Their data were consistent with the behavior of rapid-equilibrium random bireactant systems that obey Michaelis–Menten kinetics. The data also indicated that there is a synergistic effect in the binding of the two reactants at the active site, which is expressed mainly in the transition-state complex. They propose that this synergism is due to a change in the conformation of the active site in response to the binding of one of the two reactants. The K_M for Z-Phe in these coupling reactions was approximately an order of magnitude lower than the K_M for the amine component. This indicates that, if the on rates for both components are fast and comparable [as is frequently the case (Hammes & Schimmel, 1970)], then the off rate for the amine component is faster than for the carboxyl component, consistent with our proposal. Our modeling results suggest an alternative explanation for the synergism observed in the coupling reaction. In our proposed mechanism, run in reverse, the carboxyl group would change its binding orientation from a monodentate zinc ligand to bidentate as the amine component approaches its transition-state binding orientation. The Michaelis complex for the amine component may involve incomplete penetration into the active site. Consequently, both the amine and carboxyl components may change their binding orientations as the transition state is approached. The active site, however, would remain in essentially the same conformation throughout. Since a complete penetration of the amine component into the active site may be required to maximize the expression of its intrinsic binding energy, the effect on the k_{cat}/K_M by various amine components may be more dramatic than on the K_M.

The spatial arrangement of the zinc and active-site residues suggests that electrostatics may play an important role in the reaction mechanism. The zinc ion carries a net positive charge when a water molecule is coordinated in the tetrahedral ligand site. The hydrogen-bonding protons on the His-231 and Tyr-157 side chains and the zinc ion appear to create an electrostatic environment wherein the "oxyanion" of the tetrahedral intermediate should be well stabilized, analogous to the "oxyanion hole" found in serine proteases [see Asboth & Polgar (1983) and references cited therein]. Perhaps this "electropositive pocket" is also used to increase the polarization of the approaching scissile peptide and render it more reactive toward the zinc-bound water molecule. The Ala-113 backbone carbonyl and Asn-112 side-chain carbonyl dipoles along with the Glu-143 carboxylate group form a region in which a protonated amine might be stabilized. Interestingly, this "electronegative pocket" appears to be positioned to provide maximal stabilization of the protonated amine derived from the scissile peptide just after C–N bond cleavage. In our model of the reaction trajectory, the protonated Leu-Trp generated from C–N bond cleavage is in exactly the same position as the Leu-Trp fragment of the inhibitor CLT [see Monzingo & Matthews (1984)]. Consequently, the positively charged amine has moved about 1.5 Å closer to the Ala-113 and Asn-112 carbonyl oxygens during C–N bond cleavage (see Figure 7). The protonated amine is now able to hydrogen bond to Ala-113 (2.9 Å) and Asn-112 (3.0 Å) as well as form a salt bridge with the Glu-143 carboxyl group (3.0 Å). In the tetrahedral intermediate the protonated amine is able to form a salt bridge with Glu-143 (3.2 Å) but cannot form a hydrogen bond with Ala-113 (4.0 Å) or Asn-112 (4.4 Å). These observations suggest that cleavage of the C–N bond might be assisted by the Ala-113 and Asn-112 carbonyl dipoles. The magnitude of these electrostatic effects on the reaction mechanism cannot be addressed at the qualitative level of our study. However, electrostatic interactions are thought to be extremely important in enzyme reaction mechanisms (Warshel, 1981). It has been proposed that enzyme active sites function as a "supersolvent" for the transition state by arranging their dipoles to stabilize the transition state (Warshel, 1981). Our qualitative observations indicate that thermolysin may have provided a supersolvent for the transition state. A rigorous quantitative study of the electrostatic interactions discussed above should further improve our understanding of this and perhaps related zinc endopeptidases.

The partial penetration of the substrate into the active site in the Michaelis complex leaves some of the substrate intrinsic binding energy unused. This additional binding energy, available from the substrate residues on either side of the cleavage point (especially in the P_2–P_1 region), may be exploited to "pull" the scissile peptide into the transition-state supersolvent. This environment, along with the nucleophilic water molecule, may serve to destabilize the ground state and stabilize the transition state, thereby accelerating the reaction. One might expect a loss of entropy by the nucleophilic water molecule and the scissile peptide linkage as the substrate penetration proceeds due to the confinements of the active site. This entropy loss may also contribute to the rate enhancement of hydrolysis achieved by thermolysin.

Various points along the reaction pathway, in addition to the Michaelis complex and the tetrahedral intermediate, have been modeled and used in preparing an animation[9] of the entire proposed mechanism. This animation was constructed by interpolating[10] between the modeled points and was displayed by using GRAMPS (O'Donnell & Olson, 1981). This "dynamic" visualization of the mechanism provided an additional dimension in qualitatively evaluating the feasibility of the proposed trajectory for the substrate.

Relationship of the Thermolysin–CLT Complex to the Proposed Mechanism. The *N*-carboxymethyl dipeptide inhibitors of zinc peptidases have been suggested to be transition-state analogues on the basis of their high potency (Patchett et al., 1980; Maycock et al., 1981). In order to further in-

[9] D. Hangauer, G. Smith, J. Andose, B. Bush, E. Fluder, P. Gund, and E. McIntyre. A movie of this animation was presented at the Eighth Enzyme Mechanisms Conference, Pacific Grove, CA, Jan 3–5, 1983, and at a workshop on Computer Assisted Chemistry in Drug Design, Philadelphia, PA, Feb 20–23, 1983, sponsored by the Drug Information Association.

[10] The interpolation was done by Dr. G. M. Smith of Merck Sharp & Dohme Research Laboratories with an in-house computer program he has written.

vestigate this possibility, the coordinates of various points along the proposed reaction pathway for peptide cleavage were compared with the CLT–thermolysin complex. A superposition of the coordinates for bound CLT on the proposed tetrahedral intermediate is shown in Figure 7.

A number of interesting similarities and differences are seen in this comparison. One common feature is the similar positioning of the respective phenyl groups in the S_1 subsite. The zinc-coordinating oxygens of the tetrahedral intermediate and CLT also closely correspond. Finally, the Trp residues of both structures are similarly positioned in the S_2' subsite. The greatest differences occur in the parts of the structures adjacent to the zinc-binding groups. This is a consequence of the inhibitor having an "extra" bond between the zinc-binding carboxyl group and the main chain of the molecule. For this reason, the parts of CLT nearest to the zinc-binding carboxyl group are displaced (relative to the tetrahedral intermediate) away from the zinc and toward the S_2' end of the active site. The phenyl group must then enter the S_1 subsite from a different (but acceptable) angle.

As shown in Figure 10, the amine generated during peptide hydrolysis is likely to be protonated in the tetrahedral intermediate and after C–N bond cleavage. As mentioned earlier, the Leu-Trp fragment of CLT is in the same position as the Leu-Trp product just after C–N bond cleavage. Therefore, by analogy, one might expect the inhibitor amine to be protonated also. However, one should note that Glu-143 may be protonated in the CLT–thermolysin complex (Monzingo & Matthews, 1984) whereas it is likely to be ionized in the tetrahedral intermediate complex and after C–N bond cleavage. This may result in the formation of a hydrogen bond between Glu-143 and the protonated CLT amine as suggested by Monzingo & Matthews (1984). The lack of a salt bridge makes the binding of CLT as a neutral amine more plausible. However, the absence of the second amine proton would reduce the number of hydrogen bonds possible with the enzyme and position a lone pair adjacent to one or more of the three nearby carbonyl oxygens. Therefore, although definitive evidence may only come from a neutron diffraction study, it does seem likely that the amino group of CLT is protonated in the thermolysin complex.

From this comparison we suggest that the inhibitor CLT can be most accurately described as representing a point along the reaction coordinate just after the metastable tetrahedral intermediate. A considerably more detailed study, involving difficult calculations, may be required to determine if this point is near the actual transition state. However, considering the tight binding of this class of inhibitors and the positioning of the electronegative pocket that accommodates the amine derived from the scissile peptide, a late transition state (i.e., one which occurs during C–N bond cleavage) seems plausible. One might be tempted to classify these inhibitors as "biproduct" inhibitors (Byers & Wolfenden, 1973), but to do so would imply that the zinc-coordinating carboxyl group of the cleavage product prefers to chelate in a bidentate fashion. Crystallographically solved complexes with other inhibitors that coordinate to zinc via a carboxyl group (Kester & Matthews, 1977a; Bolognesi & Matthews, 1979) indicate that monodentate coordination is typical. Furthermore, this classification would suggest that the binding orientation of the amine product just after C–N bond cleavage is the same as the Michaelis complex for reverse reaction. This is not in agreement with the Michaelis complex we have proposed, which involves incomplete penetration of the amine component into the active site.

Assuming that the active site of thermolysin is a reflection of the transition state due to its relatively rigid nature (Page, 1979, 1981) and that the mechanism of peptide cleavage is similar to ACE (Holmes & Matthews, 1981), then MK-422 may be tentatively classified as a transition-state analogue as well.

Conclusions

As this work illustrates, interactive computer graphics allows one to examine very precisely the "static" structure of an enzyme and its various complexes as determined crystallographically. From the resulting observations, coupled with subsequent modeling studies, one can construct a detailed hypothesis for the mechanism by which the enzyme functions. One can then use the modeled coordinates for the various points along the reaction coordinate to prepare an animation of the proposed mechanism and view it as a "dynamic" process. Inhibitor complexes can be compared with various points along the reaction coordinate to gain insight into their binding affinity. Also, possible structural modifications that might increase the potency of these inhibitors can be explored rationally. We have, in fact, used the present study as an aid in designing thermolysin inhibitors and will report these results in a separate publication.

While conducting studies of this type, one is required to make judgments as to the energetic consequences of alterations in the structure of various complexes. The measured binding energy of a complex is the net result of an interplay of numerous intra- and intermolecular interactions as well as entropy and solvation changes. Clearly, more explicit energy calculations and further experimentation may result in additional modifications and refinements to the proposed mechanism. In the interim, the present study provides specific proposals (with coordinates) upon which such further investigations may be designed.

In the course of this study a sizable amount of substrate data has been considered and rationalized within a self-consistent detailed mechanism. Major features of the previously proposed mechanism (Kester & Matthews, 1977a; Holmes & Matthews, 1981) that are supported by the present study include the following: (1) the attack of a water molecule, activated by Glu-143 and zinc, on the carbonyl carbon to give a tetrahedral intermediate that is not covalently linked to the enzyme and (2) catalysis via a pentacoordinate zinc intermediate.

The most significant modifications and extensions suggested herein to the previously proposed mechanism are the following: (1) The substrate only partially penetrates into the active site in the Michaelis complex and does not coordinate directly to the zinc. (2) Two Michaelis complexes are possible for the substrates that were considered. These complexes differ in the conformation about the P_1 C_α–scissile peptide bond and result in an interaction of either the P_2 or P_1 side chain with the active site. (3) The tetrahedral intermediate may be attained simultaneously with full penetration into the active site. (4) As the substrate proceeds from the Michaelis complex to the transition state, the P_1' side chain undergoes a conformational change within the S_1' pocket. (5) A trajectory of approach for the scissile peptide is offered which causes the zinc-bound water molecule to move from its native position toward Glu-143 [see also Holmes & Matthews (1981)]. (6) In addition to functioning as a general base, Glu-143 may also function as a proton shuttle whereby two protons from the nucleophilic water molecule are transferred to the scissile peptide nitrogen, the last of which may trigger product release. (7) The N^ϵ-H of His-231 may function in stabilizing the transition state rather than being the proton source for the

scissile peptide nitrogen. The transition state may also be stabilized by the O-H of Tyr-157. (8) A specific sequence of events leading from the tetrahedral intermediate to released products (in a preferred order) and native enzyme is suggested. (9) The role of electrostatics in the proposed reaction mechanism is suggested.

Acknowledgments

We gratefully acknowledge the technical support provided by the Scientific Information Department of Merck Sharp & Dohme Research Laboratories, especially Drs. B. Bush and G. Smith. We also thank Dr. A. A. Patchett for encouragement and support during the course of this study.

Registry No. CLT, 76400-07-2; TLN, 9073-78-3; Z-Phe-Phe-Leu-Trp, 92398-16-8.

References

Argos, P., Garavito, R. M., Eventoff, W., Rossmann, M. G., & Bränden, C. I. (1978) *J. Mol. Biol. 126*, 141.

Argos, P., Garavito, R. M., Eventoff, W., & Rossmann, M. G. (1981) *Biomol. Struct. Conform. Funct., Evol., Proc. Int. Symp., 1978 1*, 205.

Asboth, B., & Polgar, L. (1983) *Biochemistry 22*, 117.

Bizzozero, S. A., & Dutler, H. (1981) *Bioorg. Chem. 10*, 46.

Blaney, J. M., Weiner, P. K., Dearing, A., Kollman, P. A., Jorgensen, E. C., Oatley, S. J., Burridge, J. M., & Blake, C. C. F. (1982a) *J. Am. Chem. Soc. 104*, 6424.

Blaney, J. M., Jorgensen, E. C., Connolly, M. L., Ferrin, T. E., Langridge, R., Oatley, S. J., Burridge, J. M., & Blake, C. C. F. (1982b) *J. Med. Chem. 25*, 785.

Bolognesi, M. C., & Matthews, B. W. (1979) *J. Biol. Chem. 254*, 634.

Bush, B. L. (1984) *Comput. Chem. 8*, 1.

Byers, L. D., & Wolfenden, R. (1973) *Biochemistry 12*, 2070.

Deslongchamps, P. (1977) *Heterocycles 7*, 1271.

Fersht, A. (1977) in *Enzyme Structure and Mechanism*, W. H. Freeman, San Francisco.

Gund, P., Hangauer, D. G., Andose, J. D., Bush, B. L., Fluder, E. M., McIntyre, E. F., & Smith, G. M. (1984) *Ann. N.Y. Acad. Sci.* (in press).

Hammes, G. G., & Schimmel, P. R. (1970) in *The Enzymes* (Boyer, P. D., Ed.) Vol. II, pp 67–114, Academic Press, New York.

Hammond, J. (1955) *J. Am. Chem. Soc. 77*, 334.

Hansch, C., Li, R., Blaney, J. M., & Langridge, R. (1982) *J. Med. Chem. 25*, 777.

Holmes, M. A., & Matthews, B. W. (1981) *Biochemistry 20*, 6912.

Holmes, M. A., & Matthews, B. W. (1982) *J. Mol. Biol. 160*, 623.

Horrocks, W. D., Jr., & Sudnick, D. R. (1981) *Acc. Chem. Res. 14*, 384.

Jencks, W. P. (1980) in *Chemical Recognition in Biology* (Chapeville, F., & Haenni, A.-L., Eds.) pp 3–25, Springer-Verlag, New York.

Jencks, W. P. (1981) *Proc. Natl. Acad. Sci. U.S.A. 78*, 4046.

Jones, T. A. (1978) *J. Appl. Crystallogr. 11*, 268.

Kester, W. R., & Matthews, B. W. (1977a) *Biochemistry 16*, 2506.

Kester, W. R., & Matthews, B. W. (1977b) *J. Biol. Chem. 252*, 7704.

Langridge, R., Ferrin, J. E., Kuntz, I. D., & Connolly, M. L. (1981) *Science (Washington, D.C.) 211*, 661.

Lipscomb, W. N. (1982) *Acc. Chem. Res. 15*, 232.

Matsubara, H., Singer, A., Sasaki, R., & Jukes, T. H. (1965) *Biochem. Biophys. Res. Commun. 21*, 242.

Matsubara, H., Sasaki, R., Singer, A., & Jukes, T. H. (1966) *Arch. Biochem. Biophys. 115*, 324.

Maycock, A. L., DeSousa, D. M., Payne, L. G., ten Broeke, J., Wu, M. T., & Patchett, A. A. (1981) *Biochem. Biophys. Res. Commun. 102*, 963.

Meyer, E. F., Jr. (1980) in *Drug Design* (Ariëns, E. J., Ed.) Vol. IX, pp 267–298, Academic Press, New York.

Monzingo, A. F., & Matthews, B. W. (1984) *Biochemistry* (preceding paper in this issue).

Morgan, G., & Fruton, J. S. (1978) *Biochemistry 17*, 3562.

Morihara, K., & Tsuzuki, H. (1970) *Eur. J. Biochem. 15*, 374.

O'Donnell, T. J., & Olson, A. J. (1981) *Comput. Graphics 15*, 133.

Oyama, K., Kihara, K., & Nonaka, Y. (1981) *J. Chem. Soc., Perkin Trans. 2*, 356.

Page, M. (1979) *Int. J. Biochem. 10*, 471.

Page, M. I. (1980) *Int. J. Biochem. 11*, 331.

Page, M. (1981) *Chem. Ind. (London)*, 144.

Pank, M., Kirret, O., Paberit, N., & Aaviksaar, A. (1982) *FEBS Lett. 142*, 297.

Patchett, A. A., Harris, E., Tristram, E. W., Wywratt, M. J., Wu, M. T., Taub, D., Peterson, E. R., Ikler, T. J., ten Broeke, J., Payne, L. G., Ondeyka, D. L., Thorsett, E. D., Greenlee, W. J., Lohr, N. S., Hoffsommer, R. D., Joshua, H., Ruyle, W. V., Rothrock, J. W., Aster, S. D., Maycock, A. L., Robinson, F. M., Hirshmann, R., Sweet, C. S., Ulm, E. H., Gross, D. M., Vassil, T. C., & Stone, C. A. (1980) *Nature (London) 288*, 280.

Schechter, I., & Berger, A. (1967) *Biochem. Biophys. Res. Commun. 27*, 157.

Smith, R. N., Hansch, C., Kim, K. H., Omiya, B., Fukumura, G., Selassie, C. D., Jow, P. Y. C., Blaney, J. M., & Langridge, R. (1982) *Arch. Biochem. Biophys. 215*, 319.

Thomas, K. A., Smith, G. M., Thomas, J. B., & Feldmann, R. J. (1982) *Proc. Natl. Acad. Sci. U.S.A. 79*, 4843.

Warshel, A. (1981) *Acc. Chem. Res. 14*, 284.

Wayne, S. I., & Fruton, J. S. (1983) *Proc. Natl. Acad. Sci. U.S.A. 80*, 3241.

Weaver, L. H., Kester, W. R., & Matthews, B. W. (1977) *J. Mol. Biol. 114*, 119.

Wipff, G., Dearing, A., Weiner, P. K., Blaney, J. M., & Kollman, P. A. (1983) *J. Am. Chem. Soc. 105*, 997.